

On the mechanism of gray scale patterning of Ag-containing As_2S_3 thin films

A. Kovalskiy^{a,*}, H. Jain^a, J. Neilson^a, M. Vlcek^b, C.M. Waits^c, W. Churaman^c, M. Dubey^c

^aCenter for Optical Technology, Materials Science and Engineering Department, Lehigh University, 5 E Packer Ave., Bethlehem, PA 18015, USA

^bDepartment of General and Inorganic Chemistry, University of Pardubice, 53210 Pardubice, Czech Republic

^cUS Army Research Laboratory, Adelphi, MD 20783-1197, USA

Abstract

We demonstrate an application of photo-induced silver diffusion into chalcogenide glass thin film for gray scale lithography. The gray scale chalcogenide glass masking layer generated in the present experiments was dry etched using reactive ion etching. The etching rate increases almost linearly with the total dose of absorbed light, thus forming the basis of gray scale lithography. Chemical composition as well as electronic structure on the surface of chalcogenide glassy film has been determined by high-resolution X-ray photoelectron spectroscopy (XPS) of the film at different stages of the patterning process. Influence of thermal annealing of chalcogenide film before Ag deposition has been investigated using scanning electron microscopy (SEM) and XPS techniques. It is observed that thermal annealing of the chalcogenide film slows the process of silver diffusion during the proposed processing procedure. A mechanism is proposed to explain the stages of gray scale lithography based on chalcogenide glass photoresists.

© 2007 Elsevier Ltd. All rights reserved.

Keywords: A. Amorphous materials; A. Thin films; C. Photoelectron spectroscopy; D. Diffusion; D. Microstructure

1. Introduction

The unique phenomenon of photo-induced silver diffusion into As- and Ge-based chalcogenide glass (ChG) thin films [1] is one of the promising directions in modern lithography for the development of two-dimensional (2D) submicron size patterns [2–4]. Generally, the ChG structure lacks the macro-molecular units in the covalent bonded matrix, which should allow, in principle, a resolution of etched patterns in the range of a few nanometers. As an example, electron-beam-induced patterning of Ag/ChG bilayers with 35 nm lines has been demonstrated [5], whereas our recent results on arsenic sulfide films have demonstrated ~ 7 nm wide lines. However, when using light irradiation for pattern writing, the resolution is restricted by the limits of optical diffraction. Consequently, the minimum resolution of 2D patterns in photo-induced silver diffusion is limited to several hundred nanometers [6]. The photo-induced silver diffusion can be used for fabricating

three-dimensional (3D) gray scale masks in advanced micro-electromechanical systems (MEMS) and microelectronic technologies [7]. The smooth 3D microstructures in the ChG film can be transferred to Si by dry etching more accurately than with polymers used in traditional lithography owing to the higher hardness of the glass. An understanding of the microstructural mechanism for photo-induced silver diffusion as well as the influence of chemical treatment and dry etching are extremely important for the development of this technology. Therefore, in this work we investigated the structural evolution at the surface of arsenic sulphide thin films accompanying the photodiffusion of silver by high-resolution X-ray photoelectron spectroscopy (XPS) and scanning electron microscopy (SEM). To have a better controlled diffusion profile, we compare the photodiffusion mechanisms and microstructures of as prepared and annealed ChG films.

2. Gray scale lithography

For lithographic purposes amorphous Ag/ As_2S_3 thin film bilayer samples were prepared by thermal evaporation

*Corresponding author. Tel.: +1 610 758 6879.

E-mail address: ank304@lehigh.edu (A. Kovalskiy).

method. First, As_2S_3 films (300–500 nm thickness) were deposited on Si wafers from the bulk glass (amorphous materials Inc.), followed by the deposition of a silver layer (20–50 nm). To minimize oxygen contamination the vacuum chamber was purged with Ar before glass evaporation. Details can be found in Ref. [2].

The thin film samples were irradiated with a halogen lamp (fiber-lite PL-illuminator, Dolan–Jenner Industries) through a HEBS glass calibration plate (HEBS5) from canyon materials consisting of gray scale motives with gradual smooth change of transparency as well as lens-like structures. The time of exposure was varied widely from 1 to 200 min. After exposure, the residual undiffused silver was removed from unexposed parts using dilute HNO_3 .

Dry etching was carried out with a conventional system (Plasma Therm SSL-720) using CF_4 as the etchant gas, with pressure of 100 mTorr, an electrode power of 110 W, CF_4 flow rate of 100 sccm and an etching time of 2 min. Pieces of the samples were mounted on unmasked 4-in Si wafer substrates using thermal grease (Cool-Grease TM 7016, AI Technology Inc.) in order to utilize the load lock on the RIE system. Such reactive ion etching (RIE) is widely used in submicron lithography because of the possibility of all dry process. The variation of etch depth was measured and imaged using a VEECO NT1100 Optical Profiler.

It is well known that photodiffusion of silver into ChG thin films significantly changes (usually increases) the chemical reactivity of the material [4]. Gray scale lithography in ChG is based on the fact that not only exposure time, but light intensity too affects the etching rate. Fig. 1 demonstrates the dependence of etched depth on the transparency of the gray scale features in the mask, which was uniformly exposed by halogen lamp light. The optical density through the HEBS glass mask ranged from 0.126 (shallowest etch of 65 nm) to 0.217 (deepest etch of 230 nm) allowing the intensity incident on the ChG surface to vary accordingly. This dependence is nearly linear, thus demonstrating a uniform diffusion of silver to different depths that depend on the dose of irradiation. So a smooth shaping of more complex patterns from the gray scale optical mask could be expected. The selectivity of the

etching (defined as the etching rate ratio of exposed and unexposed material) is a function of thin layer composition, its prehistory as well as of etching gas composition. In our experiment, the etching depth was 200 nm, although greater values are possible [8].

Step-like character of Ag depth profile, observed by Rutherford backscattering spectroscopy [8] suggests that some chemical reaction controls diffusion of the Ag inside the glass matrix. At the same time, easy light-induced ionization of Ag layer indicates that photogenerated holes also contribute to the Ag^+ migration process [9].

An example of smooth, lens-like patterns is shown in Fig. 2. This negative image was obtained by photodiffusion of silver followed by dry etching with CF_4 plasma. It clearly illustrates the possibility of smooth shaping of ChG films by the present method. The deep rings in Fig. 2 represent the edges where silver accumulates and the etching is much slower—the so-called sharp edge effect [2]. The same effect was observed by us earlier in 2D patterning [2]. This phenomenon was explained previously by Ag accumulation because of its lateral diffusion [2,4]. Possible ways to eliminate sharp edges are connected with the change of temperature, composition of the layers, intensity of illumination and also on electrical conductivity of the substrate [10].

3. Surface chemistry of freshly deposited ChG

Inspection of surface chemistry using high-resolution XPS is one of the most effective ways for optimizing the patterning process. Concentration of homopolar bonds in the freshly deposited As_2S_3 thin film, the interaction of Ag layer with ChG matrix before and during the exposure, chemical consequences of removal of the remaining Ag in dilute HNO_3 are some of the important parameters, which need to be assessed for this purpose [2].

The XPS core level spectra were obtained using Scienta ESCA-300 spectrometer with monochromatic Al K_α X-rays (1486.6 eV). The experimental procedure can be found in Ref. [2]. The analysis of As 3d and S 2p core level spectra of freshly deposited As_2S_3 400-nm thick film confirm the chemical composition as close to stoichiometric value (37.5 at% As, 62.5 at% S), with the fraction of oxygen on the surface as ~9 at%. The As 3d curve fitting required at least two components each consisting of individual spin–orbit doublet: one of them (~85% of all As atoms) corresponds to As within $\text{AsS}_{3/2}$ pyramidal units and the other component (~15% of all As atoms) is attributed to As within As–As homopolar bonds. Similarly, fitting of S 2p core level suggest at least two doublet components: 93% of all S atoms within $\text{AsS}_{3/2}$ and 7% within “wrong” S–S bonds. Arsenic oxide (As_2O_3 or As_2O_5) is not detected during the time after deposition. Oxygen, when present, exists in the form of hydroxide complexes or physisorbed on the ChG substrate; discussion of this topic is the subject of a separate detailed analysis.

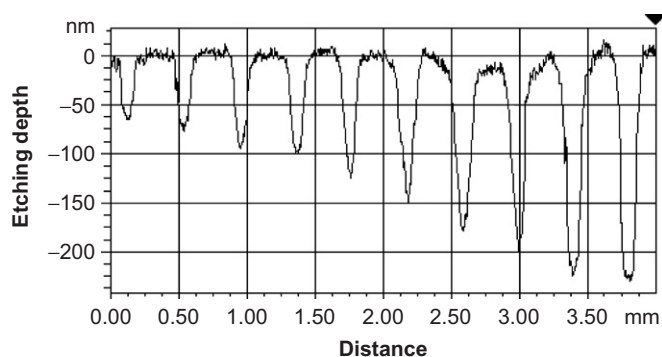


Fig. 1. Profilogram demonstrating the change of etching depth with gradual variation of transparency of mask fragments.

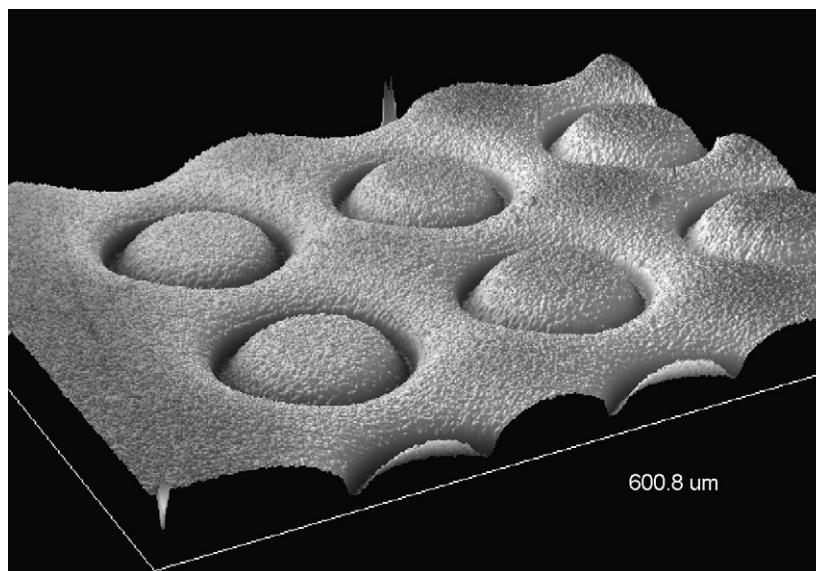


Fig. 2. Negative optical profiler image demonstrating the fabrication of smooth lens-like mask by photoinduced Ag diffusion into As_2S_3 film followed by dry etching (total etched depth ~ 200 nm).

To study the influence of light illumination (halogen lamp, 15 mW/cm^2) on the efficiency of Ag interaction with ChG thin film, the exposed and unexposed samples of Ag/ As_2S_3 bilayers were placed in the high vacuum (HV) XPS chamber after the removal of excess Ag. As seen from Fig. 3, significant chemical shift takes place when we compare the core level spectra of As 3d, S 2p and O 1s, while no changes are observed at Ag $3d_{5/2}$. Difference in the values and sign of chemical shift for various core levels confirms genuine changes in the structure rather than surface charging.

As/S ratio for unexposed sample after Ag removal (in dilute HNO_3) decreases slightly in comparison with the freshly prepared ChG film (0.56 instead of 0.60). The fraction of oxygen is twice as much as in the unexposed As_2S_3 (19 at%) and the fraction of silver is ~ 3.5 at%. It means that HNO_3 acts as a solvent not only for pure Ag but also for some type of As-enriched fragments. Fitting of As 3d core level spectrum shows almost a complete disappearance of the As–As bonds and formation of arsenic oxide (~ 16 at% of all As sites).

Irradiation leads to the further decrease of As concentration after HNO_3 treatment ($\text{As/S} = 0.48$), with concentration of oxygen and Ag being 20 and 12 at%, respectively. An additional experiment with prolonged light irradiation gives $\text{As/S} = 0.30$ ratio. Taking into account of the preferable bonding of Ag with S, apparently As-rich clusters are formed upon irradiation, which are either oxidized or washed out by the acid.

The structure of S 2p core level is more complicated. For both unexposed and exposed samples, after Ag removal one observes a distinct “tail” at higher binding energies (Fig. 3). Usually such a feature is associated with S–O complexes. In the present case, such complexes are formed possibly as part of some sulfur-containing acid

products of reaction of As_2S_3 matrix and Ag with dilute HNO_3 .

The core level spectra of As and S shows that after the HNO_3 treatment significantly more As–O chemical bonds are left behind on the surface of unexposed bilayer than of the surface of the irradiated samples, although the concentration of oxygen remains close to 20% in both cases.

At first, from the absence of the chemical shift of Ag $3d_{5/2}$ core level (Fig. 3), it appears that silver forms the same compound with sulfur in both the exposed and unexposed regions. However, a detailed analysis of S 2p core level peaks reveals two different Ag-containing S environments in the unexposed region (e.g. Ag_2S and another relatively Ag-poor phase). In the exposed sample only the latter phase is observed. As a result of silver photodiffusion, the formation of such an Ag-containing surface layer was also proposed previously by other authors [8]. At the same time, the coincidence of the Ag $3d_{5/2}$ core level components for both exposed- and unexposed-samples testifies that the character of Ag bonding with S in these separated fragments should be the same as in non phase-separated structural units.

4. Influence of ChG annealing

The annealing of ChG films at just below the glass transition temperature (T_g) in vacuum is commonly used to stabilize its structure and properties [11]. It usually decreases the defect concentration and improves structural homogeneity. Annealing of the ChG films before Ag deposition in our lithography process is attractive for higher reproducibility. Also we hoped that it may decrease lateral diffusion and overcome the sharp edge formation mentioned earlier.

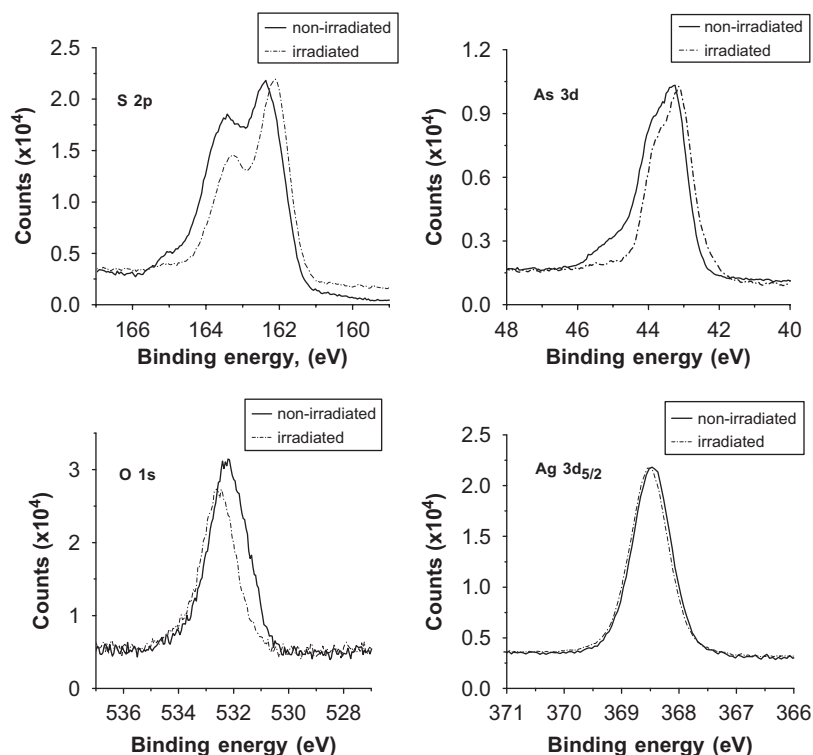


Fig. 3. Comparison of XPS core level spectra of bilayers Ag/As₂S₃ (non-irradiated and irradiated by halogen lamp, $W = 15 \text{ mW/cm}^2$) after removing of Ag layer in dilute HNO₃.

For annealing studies, 400-nm thick As₂S₃ films were deposited on Si substrate, and annealed in vacuum at 175 °C. Next, a Ag layer (40 nm) was deposited on top of both annealed-and non-annealed ChG films. Then Ag was removed from both films by dissolving in dilute HNO₃. One of the samples was placed in a SEM (JEOL 6300F FE-SEM, 2 keV) to study the film surface after Ag removal. The other sample was placed in XPS chamber to study the chemical composition of the surfaces.

SEM pictures (Fig. 4a) clearly demonstrate the accumulation of some part of Ag as a separate phase on the annealed ChG film surface after HNO₃ treatment. The formation of silver compound is further confirmed by the significant chemical shift between the core level peaks of pure Ag and new compound, revealed by high resolution XPS. Such phenomenon is not observed in non-annealed film, where undissolved silver immediately diffuses into ChG film under e(electron)-beam action. This observation of a much faster dissolution of Ag in the ChG matrix of non-annealed film than in the annealed films is obviously very important for our lithography applications.

The reason for the accumulation of Ag on the annealed film surface could be partial polymerization of S chains near the surface region, which are supposed to be the main source of S for forming new Ag–S bonds. Earlier similar explanation of induction period for silver diffusion in ChG was presented in Ref. [9]. Polymerization could also be the reason for a much lower S/As ratio (2.75) after Ag removal

in dilute HNO₃ in comparison with its value for non-annealed film (6.80). So, the concentration of these S–S chains becomes too low to provide effective driving force for the dissolution of Ag ions under the influence of electron beam.

The dynamics of further transformations of Ag-containing phase in the annealed As₂S₃ film under electron irradiation are shown in Figs. 4b–d. This process can be interpreted as electron-induced Ag accumulation with participation of lateral diffusion [12] followed by Ag dissolution. After 5 min of electron irradiation there is no evidence of phase separation or Ag accumulation in the SEM micrographs (see Fig. 4d). So, we can conclude that at this stage of electron-induced Ag diffusion the submicron-size phase separated regions have disappeared and a homogeneous Ag-containing phase has developed. Obviously, this method of observation is limited to the surface, and we cannot exclude the formation of phase separated regions inside the sample.

Comparing the As 3d and S 2p core level spectra for non-annealed and annealed ChG films after removing the silver layer in dilute HNO₃ (Fig. 5), we conclude that the changes in As peak are due to the decrease in concentration of arsenic oxide in annealed ChG. Furthermore, the S 2p spectrum shows that the ratio of the concentrations of As–S and Ag–S bonds is changing, confirming the formation of Ag-enriched surface layer in the annealed sample.

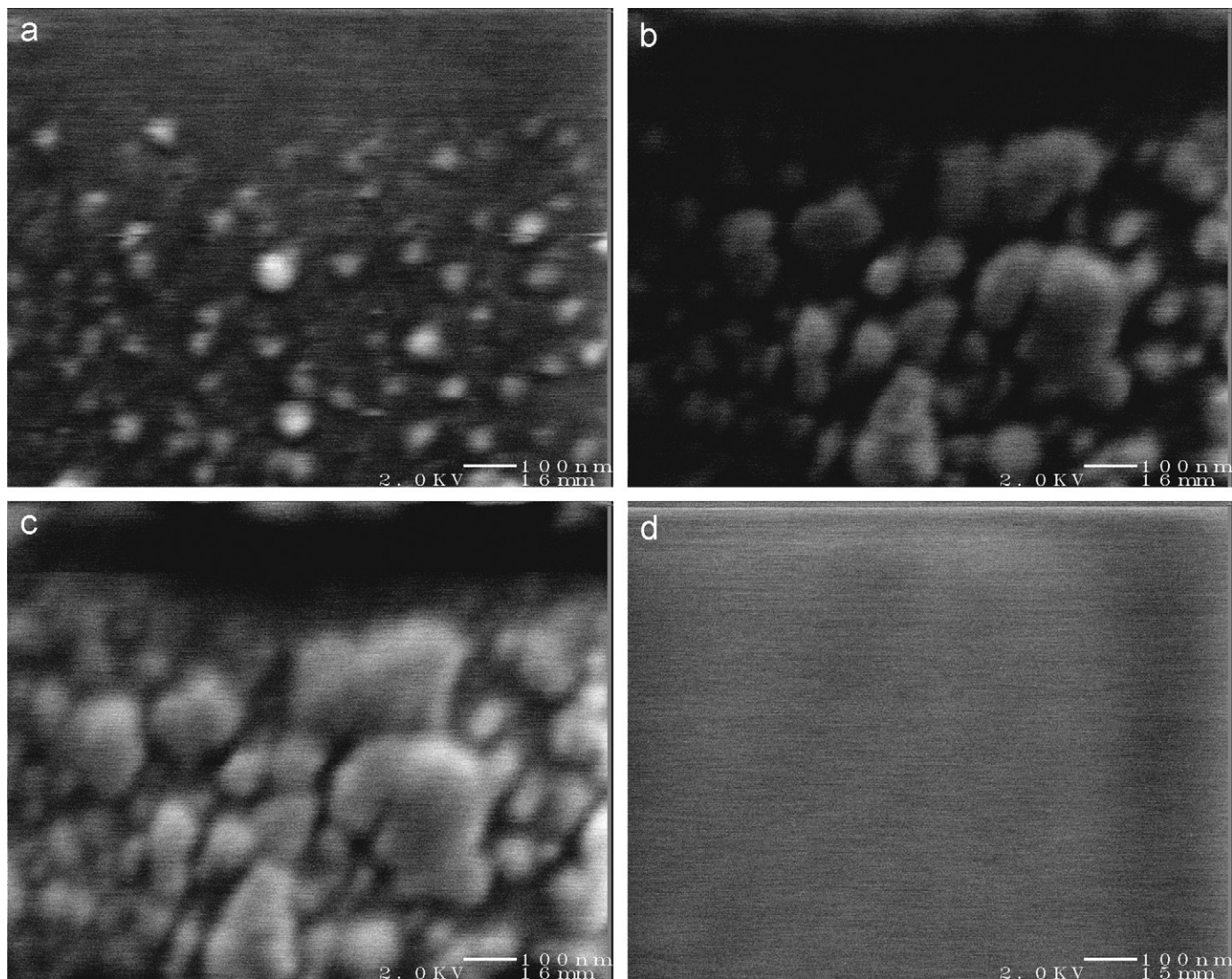


Fig. 4. SEM pictures ($\times 100,000$) of annealed As_2S_3 thin films after removing of Ag from the surface in dilute HNO_3 : a—fresh sample; b—1 min, c—2 min, d—5 min of electron irradiation.

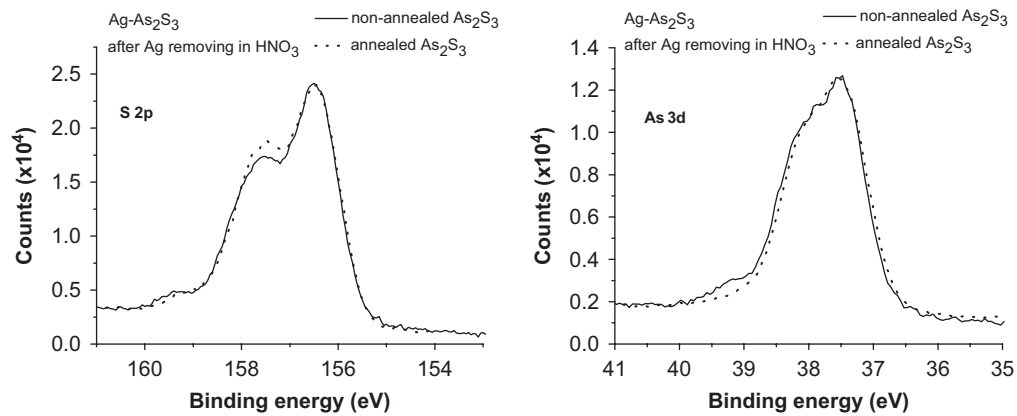


Fig. 5. Comparison of XPS core level spectra of bilayers $\text{Ag}/\text{As}_2\text{S}_3$ for chalcogenide glass films non-annealed and annealed at 20 K below glass transition temperature T_g .

5. Conclusions

The well-known phenomenon of photo-induced silver diffusion into chalcogenide glass can be effectively used in modern lithography for gray scale micropatterning. Nearly linear dependence of the etch depth on the amount of absorbed light suggests that high-quality 3D patterning can be accomplished by dry etching. However, the problem of sharp edge formation remains to be resolved. XPS data indicate that not only silver layer but also As rich fragments in the film are removed by dilute HNO_3 , thus substantially influencing the patterning process. Additional thermal annealing of ChG film before Ag deposition slows the process of silver diffusion inside of ChG. This phenomenon is explained by partial polymerization of S chains in near surface region.

Acknowledgments

Separate parts of this work were supported by a Lehigh University—Army Research Lab (ARL) collaborative research program, and the National Science Foundation (DMR 00-74624, DMR 03-12081, DMR 04-09588).

References

- [1] A.V. Kolobov, S.R. Elliott, Photodoping of amorphous chalcogenides by metals, *Adv. Phys.* 40 (1991) 625–684.
- [2] A. Kovalskiy, M. Vlcek, H. Jain, A. Fiserova, C.M. Waits, M. Dubey, Development of chalcogenide glass photoresists for gray scale lithography, *J. Non-Cryst. Solids* 352 (2006) 589–594.
- [3] N.P. Eisenberg, M. Manevich, M. Klebanov, V. Lyubin, S. Shtutina, Fabrication and testing of microlens arrays for the IR based on chalcogenide glassy resists, *J. Non-Cryst. Solids* 198–200 (1996) 766–768.
- [4] M.N. Kozicki, S.W. Hsia, A.E. Owen, P.J.S. Ewen, PASS—a chalcogenide-based lithography scheme for I.C. fabrication, *J. Non-Cryst. Solids* 137–138 (1991) 1341–1344.
- [5] G.H. Bernstein, W.P. Liu, Y.N. Khawaja, M.N. Kozicki, D.K. Ferry, L. Blum, High-resolution electron beam lithography with negative organic and inorganic resists, *J. Vac. Sci. Technol. B* 6 (1988) 2298–2302.
- [6] K.L. Tai, R.G. Vadimsky, C.T. Kemmerer, J.S. Wagner, V.E. Lamberti, A.G. Timko, Submicron optical lithography using an inorganic resist/polymer bilevel scheme, *J. Vac. Sci. Technol.* 17 (1980) 1169–1176.
- [7] C.M. Waits, B. Morgan, M.J. Kastantin, R. Ghodssi, Microfabrication of 3D silicon MEMS structures using gray-scale lithography and deep reactive ion etching, *Sensors Actuat. A* 119 (2005) 245–253.
- [8] T. Wagner, A. Mackova, V. Perina, E. Rauhala, A. Seppala, S.O. Kasap, M. Frumar, Mir. Vlcek, Mil. Vlcek, The study of photo- and thermally-induced diffusion and dissolution of Ag in $\text{As}_{30}\text{S}_{70}$ amorphous films and its reaction products, *J. Non-Cryst. Solids* 299–302 (2002) 1028–1032.
- [9] K. Tanaka, Photoelectronic process of photodoping in the Ag/As–S system, *J. Appl. Phys.* 70 (1991) 7397–7402.
- [10] T. Wagner, M. Frumar, V. Suskova, Photoenhanced dissolution and lateral diffusion of Ag in amorphous As–S layers, *J. Non-Cryst. Solids* 128 (1991) 197–207.
- [11] P. Boolchand, R.N. Einzweiler, M. Tenhover, Structural ordering of evaporated amorphous chalcogenide film alloys: role of thermal annealing, *Diffus. Defect Data* 53–54 (1987) 415–420.
- [12] N. Yoshida, K. Tanaka, Ag migration in Ag–As–S glasses induced by electron-beam irradiation, *J. Non-Cryst. Solids* 210 (1997) 119–125.